Journal of Power Sources 196 (2011) 110–115

Contents lists available at ScienceDirect

Journal of Power Sources

journal homepage: www.elsevier.com/locate/jpowsour

Sub-nano-Pt cluster supported on graphene nanosheets for CO tolerant catalysts in polymer electrolyte fuel cells

EunJoo Yoo[a], Tatsuhiro Okada[a], Tomoaki Akita[c], Masanori Kohyama[c], Itaru Honma[b,*], Junji Nakamura[a,**]

[a] Graduate School of Pure and Applied Science, University of Tsukuba, Tsukuba, Ibaraki 305-8573, Japan
[b] Energy Technology Research Institute, National Institute of Advanced Industrial Science and Technology, 1-1-1 Umezono, Central 2, Tsukuba, Ibaraki 305-8568, Japan
[c] Research Institute for Ubiquitous Energy Devices, National Institute of Advanced Industrial Science and Technology, 1-8-31 Midorigaoka, Ikeda 563-8577, Japan

ARTICLE INFO

Article history:
Received 18 March 2010
Received in revised form 25 June 2010
Accepted 8 July 2010
Available online 15 July 2010

Keywords:
Sub-nano-Pt clusters
Graphene nanosheet
CO tolerance

ABSTRACT

The carbon monoxide (CO) tolerance performance of polymer electrode fuel cells (PEFCs) was studied for a catalyst composed of graphene nanosheets (GNS) with sub-nano-Pt clusters. The Pt catalysts supported on the GNS showed a higher CO tolerance performance in the hydrogen oxidation reaction (HOR), which was significantly different from that of platinum on carbon black (Pt/CB). It is proposed that the presence of the sub-nano-Pt clusters promotes the catalytic activity and that the substrate carbon material alters the catalytic properties of Pt via the interface interactions between the graphene and the Pt.

1. Introduction

Graphene nanosheets (GNS) are promising carbon materials for a variety of energy technologies, including electrocatalysis, lithium ion batteries, hydrogen storage and capacitors. This is because they exhibit unique two-dimensional sheet structures and superior electrical conductivities when compared with graphitic carbon. GNS are obtained by the chemical reduction of graphite and are used for large scale applications [1–6]. We have reported that GNS exhibit giant Li-ion intercalation capacities reaching 784 mAh/g, in a reversible way, which is more than twice that of graphite [1,2]. Several groups have reported that metal nanoparticles such as Pt and Au, when supported on GNS, show high performances when used as electrocatalysts for fuel cells [3–7]. The enhanced performance of the electrocatalyst is attributed to the high specific surface area of the GNS. We have also reported that Pt catalysts supported on GNS show a high performance for methanol oxidation reaction (MOR) when compared with Pt/carbon black (Pt/CB). It has been suggested that this high performance for MOR is attributed to the formation of sub-nano-Pt clusters on GNS with average sizes of 0.3 nm. Pt particles of such a small size have not previously been observed on carbon. The presence of sub-nano-Pt clusters on GNS has been thought to enhance the MOR activity [8]. It is therefore expected that GNS with sub-nano-Pt clusters will be excellent candidates for use as electrocatalysts in fuel cells. However, there have been no reports on the evaluation of electrocatalysts in polymer electrolyte fuel cells (PEFCs). Therefore, we have investigated the use of Pt/GNS as anode or cathode electrocatalysts for PEFCs. It is thought that the catalytic activity of Pt is promoted by using this new, unique carbon material, leading to a reduction in Pt usage, in PEFCs. The development of carbon monoxide (CO) tolerant catalysts is required for the commercialization of stationary type PEFCs, using hydrogen fuels produced from reforming hydrocarbons. It is widely recognized that Pt catalysts are deactivated by a small amount of CO and that Pt/Ru alloy catalysts are highly CO tolerant. We report here a catalyst composed of GNS with sub-nano-Pt clusters which show a high CO tolerance as an anode catalyst for PEFCs.

2. Experimental

Graphene nanosheets (GNS) were obtained via a solution-based route, involving the chemical oxidation of graphite to hydrophilic graphite oxide. Graphite oxides were made by the Hummers method [9]. Graphite oxides were easily exfoliated to form individual graphene oxide sheets, by ultrasonication in water. The graphene oxide sheets were then reduced to graphene nanosheets by use of hydrazine hydrate.

* Corresponding author. Tel.: +81 29 861 5648; fax: +81 29 861 5648.
** Corresponding author. Tel.: +81 29 853 5279; fax: +81 29 853 5279.
E-mail addresses: i.homma@aist.go.jp (I. Honma), nakamura@ims.tsukuba.ac.jp (J. Nakamura).

0378-7753/$ – see front matter © 2010 Elsevier B.V. All rights reserved.
doi:10.1016/j.jpowsour.2010.07.024

The 20 wt% Pt catalysts were deposited onto graphene nanosheets using a platinum precursor of $[Pt(NO_2)_2(NH_3)_2]$ (Ishifuku Metal Industry, Tokyo) in an ethanol solution. The powdered mixture was dispersed in ethanol, dried in air at 40 °C for 1 h and then subjected to heat-treatment in a hydrogen/Argon (H_2/Ar) (1:4, v:v) stream at 400 °C for 2 h in a furnace. Commercial 20 wt% Pt/CB and 20 wt% Pt-10 wt% Ru/CB catalysts (Johnson Matthey) were also tested for comparison. Transmission electron microscopy (TEM) images showed that well-dispersed Pt and Pt–Ru particles with sizes ranging from 2 to 3 nm were obtained for these commercial catalysts. The amount of Pt or Ru in the electrocatalysts was estimated by ICP (inductively coupled plasma) analysis.

The catalytic activity for a hydrogen oxidation reaction (HOR) was tested in a three-electrode glass cell, in 0.05 mol dm^{-3} H_2SO_4 at room temperature, under a flow of pure H_2 or in a mixture of 500 ppm CO/H_2, in the solution for 1 h. Catalysts were loaded onto a glassy carbon disk electrode (0.28 cm^2) with diluted (1:50 in methanol) 5 wt% Nafion solution (Aldrich). The working electrode was a catalyst supported on a glassy carbon disk, the counter electrode was a platinum plate, and a silver/silver chloride electrode (Ag/AgCl) was used as the reference electrode.

CO_{ad} oxidation was measured by CO_{ad} stripping voltammetry, in a 0.05 mol dm^{-3} H_2SO_4 solution, at room temperature. 3% CO/N_2 gas was passed into the cell for 1 h. Then, the CO/N_2 gas was purged with N_2 gas for 30 min, and the CO_{ad} stripping experiment was performed at a scan rate of 10 mV s^{-1}. The hydrogen ionization measurements of the CO_{ad}-covered electrodes were performed by bubbling hydrogen gas for 30 min, to produce a saturated solution. Cyclic voltammetry was carried out in a flow of H_2 gas at a scan rate of 10 mV s^{-1}.

A durability test was performed, with repeated potential cycling, between −0.25 and 1.0 V *vs.* Ag/AgCl at 50 mV s^{-1} in N_2 saturated 0.05 mol dm^{-3} H_2SO_4 at room temperature.

The morphological structures of the Pt/GNS and the Pt/CB were characterized by High-Angle Annular Dark-Field Scanning Transmission Electron Microscopy (HAADF-STEM, JEOL, JEM-3000F).

3. Results and discussion

The prepared GNS revealed a curled morphology, consisting of a thin wrinkled paper-like structure as shown by the SEM images in Fig. 1(a). The thickness of the GNS was estimated to be between 3 and 7 nm by SEM measurements, corresponding to *ca.* 10–20 stacked layers of monatomic graphene sheets. In addition, as shown in the TEM images in Fig. 1, the thin GNS were irregularly bent and deformed like crumpled paper, and the graphene sheets were randomly stacked. The morphological structure, the particle size, and the metal dispersion of the Pt electrocatalysts were also examined by TEM. Fig. 1(c) and (d) shows the TEM images of Pt/GNS and Pt/CB, respectively. Pt particles with sizes of 2–3 nm for the Pt/GNS and Pt/CB were well-dispersed on the GNS and the CB. To observe sub-nano-Pt clusters, HAADF-STEM images were taken for both the Pt/GNS and the Pt/CB. Fig. 1(e) shows the image of the Pt/GNS and it can be seen that platinum is finely dispersed on the GNS with many clusters being less than 0.5 nm in diameter and with the largest being 2 nm wide. The image were also used to study the size of the smaller Pt clusters and these were estimated to be 0.3 nm. However, the HAADF-STEM measurements did not show any sub-nano-Pt clusters supported on the carbon black of the Pt/CB (Fig. 1(f)).

Fig. 2 shows the catalytic activities of the Pt/GNS, Pt/CB and PtRu/CB for the HOR reaction for 1 h at room temperature in pure H_2 and in H_2 with 500 ppm CO. In pure H_2, the catalytic activities of all the samples were similar, regardless of the type of carbon material used. However, a significant support effect was observed in the presence of H_2 with 500 ppm CO. The HOR activity of the Pt/GNS electrocatalyst remained at *ca.* 52% (0.44 mA cm^{-2}) of that in pure H_2 at −0.1 V *vs.* Ag/AgCl. In contrast, the Pt/CB electrocatalyst exhibited less than about 11% (0.13 mA cm^{-2}) of the catalytic activity in H_2. In comparison, the PtRu/CB, which is a well-known CO tolerant catalyst, maintained a catalytic activity of up to 45% (0.54 mA cm^{-2}) under 500 ppm CO/H_2. This clearly shows that the CO tolerance performance of the Pt/GNS is significantly superior to that of Pt/CB and that the substrate carbon material alters the catalytic properties of the Pt for the PEFCs.

To investigate the differences in the CO tolerance performance between the Pt/GNS and the Pt/CB, we examined the relationship between the onset potentials of the hydrogen ionization and the CO oxidation potentials of all of the measured samples. Fig. 3 shows the hydrogen ionization voltammograms on CO_{ad}-covered Pt as well as the CO stripping voltammograms. The anodic current of the CO_{ad} oxidation on the Pt/GNS starts to increase at about 0.40 V *vs.* Ag/AgCl and shows an anodic peak at 0.49 V *vs.* Ag/AgCl as shown in Fig. 3(a). If the H_2 ionization occurs on the free Pt sites formed by the removal of the CO_{ad}, the H_2 ionization of the Pt/GNS proceeds at 0.40 V *vs.* Ag/AgCl. This is the point at which CO_{ad} removal begins on the Pt. However, the H_2 ionization of the Pt/GNS was initiated at a lower voltage of 0.2 V *vs.* Ag/AgCl and attained a limiting current of 0.48 V *vs.* Ag/AgCl. In contrast, the PtRu/CB and Pt/CB catalysts showed hydrogen ionization on CO_{ad}-covered electrodes began at the same time as CO_{ad} removal started, in the CO stripping voltammograms, that is, at 0.2 and 0.42 V *vs.* Ag/AgCl, respectively. Kita et al. have reported that hydrogen ionization on Pt metal takes place on an extremely small number of vacant upd (underpotential deposition)-H sites and can easily attain a limiting current. This is because the H_2 ionization takes place at the remaining free sites, following the removal of the CO_{ad} [10]. The reasons why the Pt/GNS showed such a difference in behavior towards hydrogen ionization on CO_{ad}-covered Pt are not yet clear. However, we believe that the existence of the sub-nano-Pt clusters on the GNS may allow hydrogen ionization to take place on the CO_{ad}-covered Pt, in the low over-potential regions.

Fig. 4 shows the CO oxidation charges for the Pt/CB and Pt/GNS as a function of CO concentration. The CO/H_2 gases with CO concentrations of 500 ppm, 1% and 3% were passed into the cell for 1 h. The CO/H_2 gases were then purged with N_2 gas for 30 min, and CO_{ad} stripping voltammetry was performed at a scan rate of 10 mV s^{-1} in N_2. The CO oxidation charge of the Pt/CB reached a full charge for the 500 ppm CO concentration. In contrast, we found that the CO oxidation charge of the Pt/GNS was approximately 10 times lower than that of the Pt/CB in a 500 ppm CO concentration. This indicated that the coverage of CO_{ad} on the Pt/GNS was relatively small at 500 ppm CO. The CO oxidation charge of the Pt/GNS reached a full charge at 1% CO concentration. These results suggest that the CO tolerant HOR activity of the Pt/GNS is greatly enhanced by the less reactive character of the Pt supported on GNS, toward CO adsorption.

The stability of the electrocatalysts is one of the most important factors because of the high demand for their long-term performance in fuel cells. This stability can be investigated by repeated potential cycling in acidic solution. We performed potential cycling between −0.25 and 1.0 V *vs.* Ag/AgCl at a scan rate of 50 mV s^{-1}, in N_2 saturated H_2SO_4 solution to examine the durability of both the Pt/GNS and Pt/CB towards the HOR. The electrochemically active surface area (ECSA) was estimated by the charge corresponding to the hydrogen desorption from the electrode surface [11]. The ECSAs for the Pt/GNS and Pt/CB were estimated to be 24.01 and 20.61 m^2/g Pt, respectively, before potential cycling. The reason why the ECSA of Pt for Pt/GNS is not so large is explained by the coexistence of larger Pt particles above 2 nm in size as shown in Fig. 1(c). Interestingly, the decrease in the ECSA value of the Pt/GNS is smaller than that of the Pt/CB, after potential cycling, as can be compared

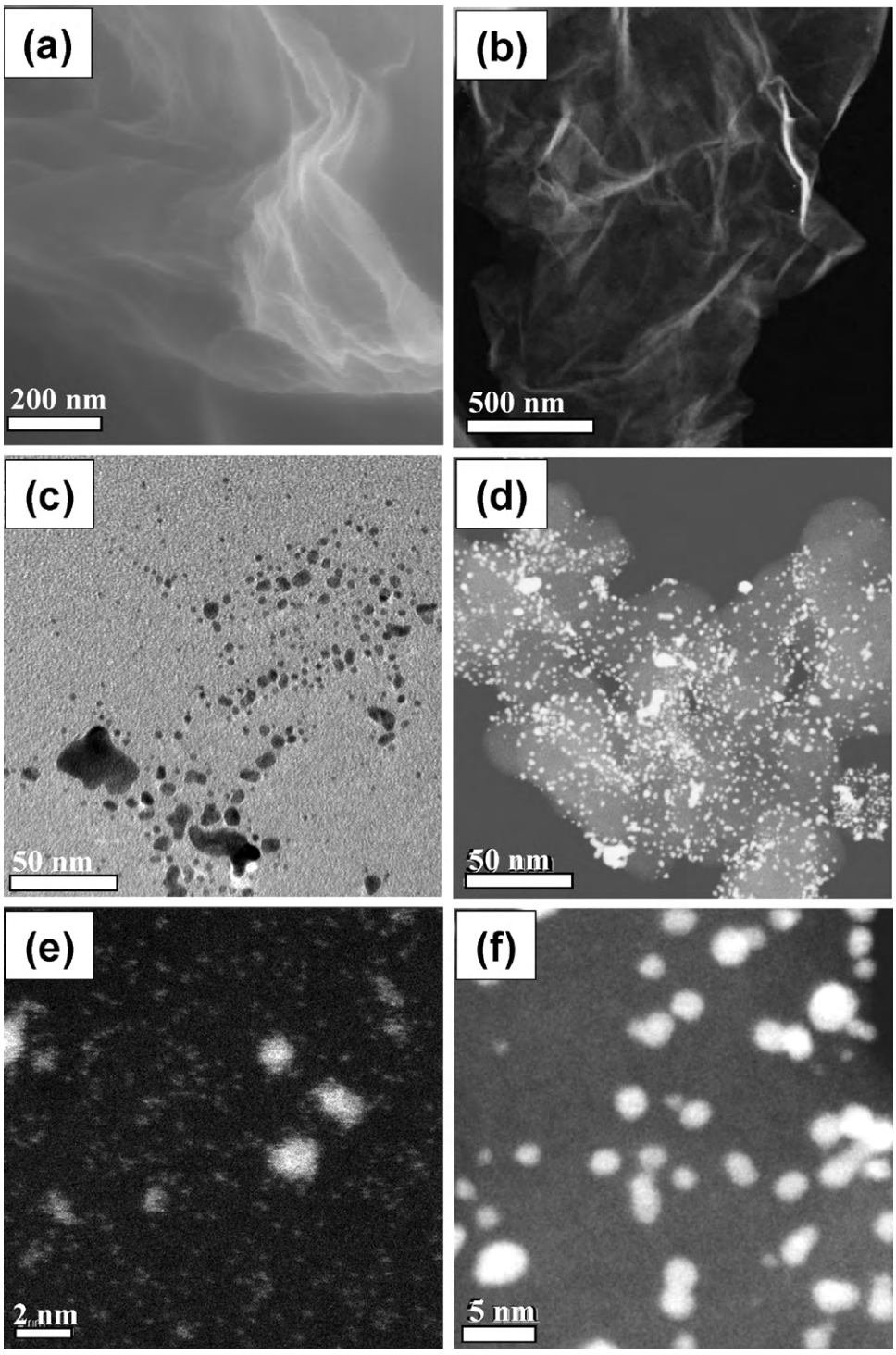

Fig. 1. SEM (a) and TEM (b) images of GNS. HAADF-STEM images of 20 wt% Pt/GNS (c) and 20 wt% Pt/CB (d). The magnification HAADF-STEM images of 20 wt% Pt/GNS (e) and 20 wt% Pt/CB (f).

in Fig. 5(a) and (b). Fig. 5(c) and (d) shows the decrease in the ECSA values with time of potential cycling. The Pt/CB lost about 75% of its initial ECSA, whereas the Pt/GNS lost only about 45% of its initial ECSA after 3000 cycles (about 21 h). Kou et al. have reported that functionalized graphene sheets, with higher numbers of π sites and functional groups, may lead to strong metal-support interactions and a resultant resistance of Pt to sintering and therefore to enhanced durability [12]. Even though both samples in our experiments lost ECSA after repeated potential cycling, the difference in the losses are considered to be due to the presence of sub-nano-Pt clusters on the GNS, with strong interactions occurring between the sub-nano-Pt clusters and the GNS. Thus, the results from these durability tests suggested that GNS are a superior substrate material on which to anchor Pt particles for use in fuel cells.

Fig. 6 shows the HOR activity of the Pt/GNS and Pt/CB in H_2, with and without 500 ppm CO, after 3000 repeated potential cycles. The HOR activity of the Pt/GNS in pure H_2 does not significantly differ from that of the initial HOR activity (0.80–0.78 mA cm^{-2}). Furthermore, the HOR activity under 500 ppm of CO/H_2 maintained *ca.* 36% of the catalytic activity in pure H_2. Conversely, the HOR activity of

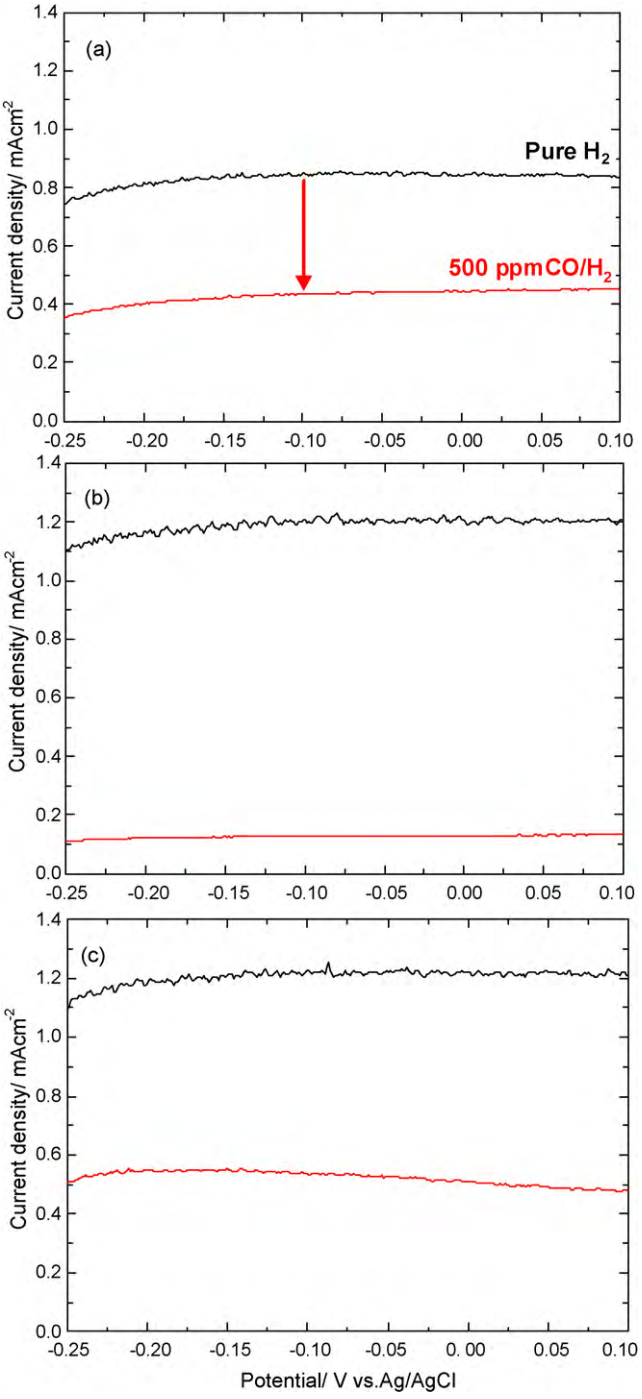

Fig. 2. Polarization curves of the hydrogen oxidation reaction on a rotating disk electrode (RDE) measured in 0.05 mol dm^{-3} H_2SO_4 at 25 °C, where H_2 gas is bubbled with and without 500 ppm CO. Rotating speed 500 rpm and scan rate 10 mV s^{-1}, (a) Pt/GNS, (b) Pt/CB and (c) PtRu/CB.

the Pt/CB in pure H_2 decreased by about 55% (1.21–0.54 mA cm^{-2}) of the initial HOR activity and stayed at 5% under 500 ppm CO/H_2. This indicates that the Pt/GNS showed a durability behavior which differed from that of the Pt/CB.

Although the mechanism of the CO tolerance for Pt/GNS is still unclear, we found that the Pt/GNS showed a significantly higher CO tolerance performance and a higher durability than that of Pt/CB. There may be two possible reasons for the excellent CO tolerant HOR activity of the Pt/GNS. First, the presence of sub-nano-Pt clusters on the GNS may promote the CO tolerance performance.

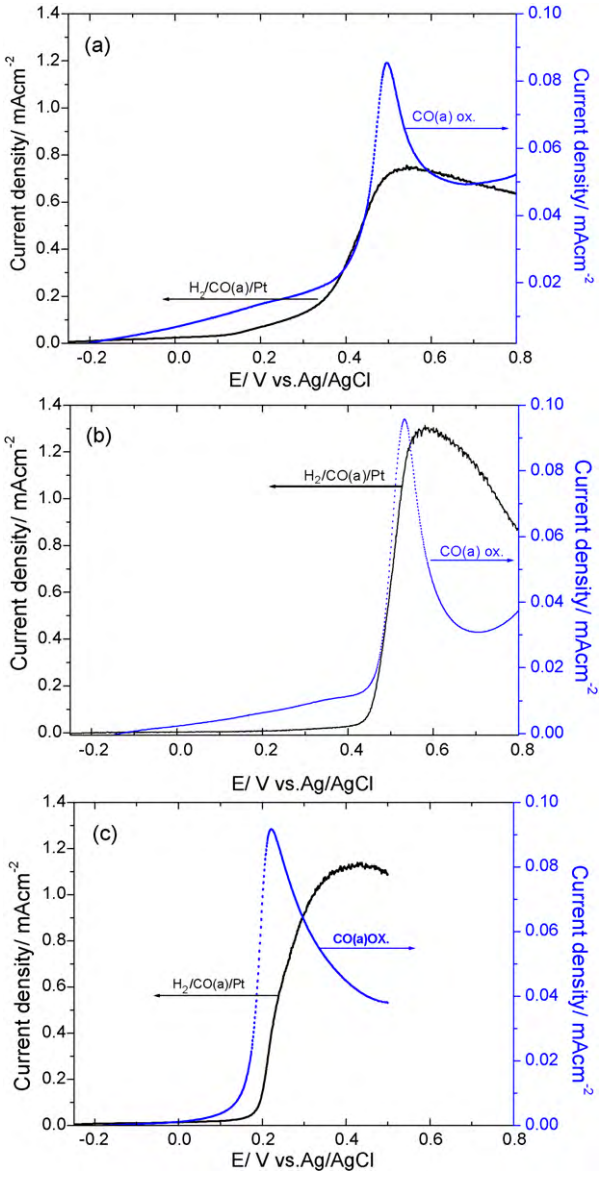

Fig. 3. The hydrogen ionization voltammogram on CO_{ad} covered Pt and CO stripping voltammogram in 0.05 mol dm^{-3} H_2SO_4 at 25 °C. (a) Pt/GNS, (b) Pt/CB and (c) PtRu/CB.

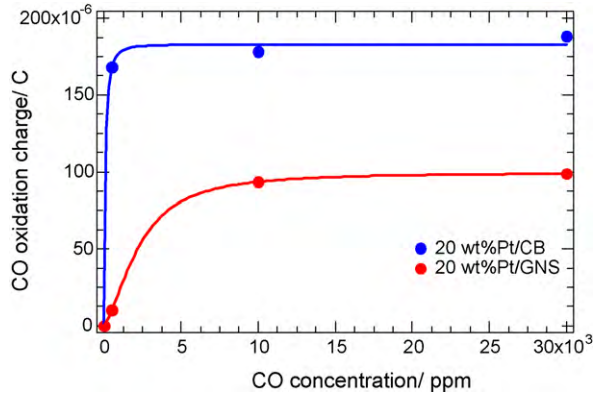

Fig. 4. The CO oxidation charges for Pt/CB and Pt/GNS as a function of CO concentration. Rotating speed 500 rpm, scan rate 10 mV s^{-1}, CO concentrations: 500 ppm, 1% and 3% CO/H_2, electrolyte: 0.05 mol dm^{-3} H_2SO_4.

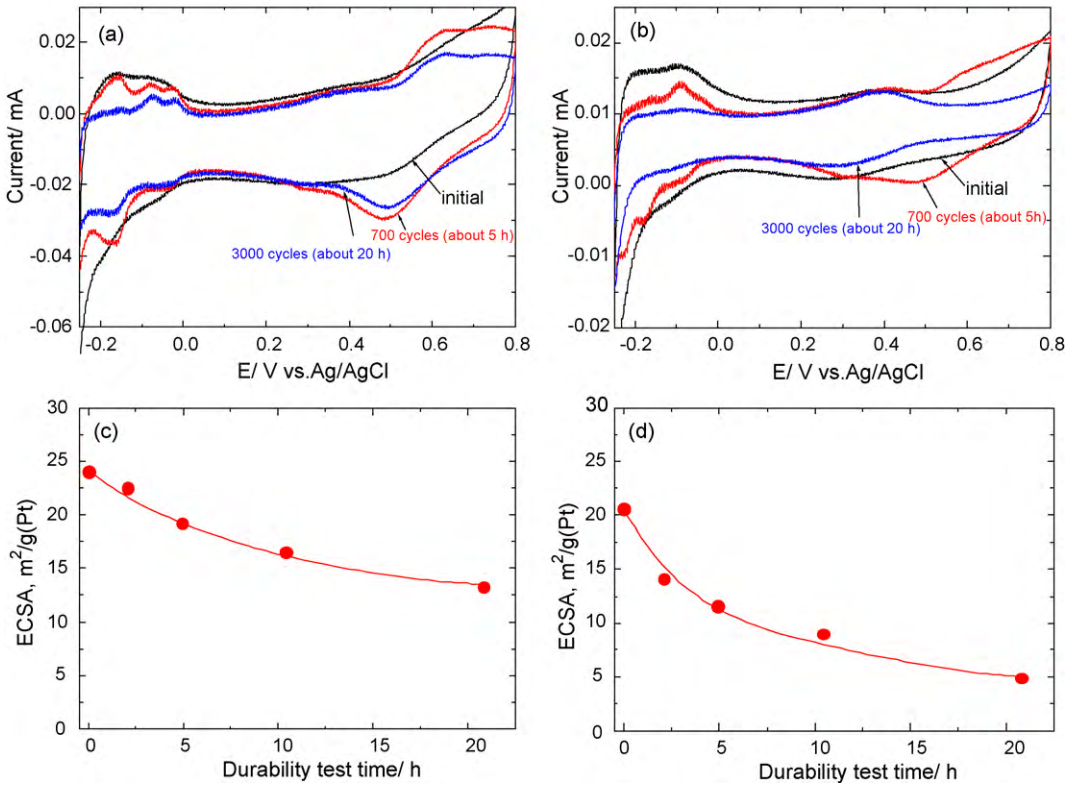

Fig. 5. Cyclic voltammograms of Pt/GNS (a) and Pt/CB (b) under a scan rate of 100 mV s^{-1} before and after 700 and 3000 CV degradation. The bottom two figures show the decay of the electrochemically active surface area of the Pt particles on GNS (c) and CB (d), during potential cycles.

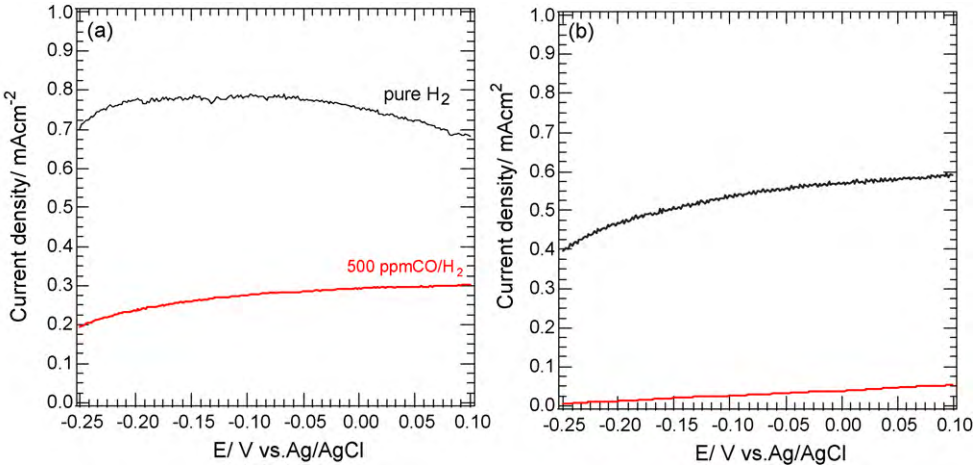

Fig. 6. Polarization curves of the hydrogen oxidation reaction after 3000 potential cycles in 0.05 mol dm^{-3} H_2SO_4 at 25 °C, where H_2 gas was with and without 500 ppm CO. Rotating speed 500 rpm and scan rate 10 mV s^{-1}, (a) Pt/GNS and (b) Pt/CB.

Second, the chemical effect due to the modification of the Pt electronic structure, by the GNS support, may cause a difference in the catalytic activities. In the previous surface science study, we have found in the case of a Pt-deposited graphite sample, that significant chemical interactions at the interface between the graphite surface and the Pt catalyst particles leads to modifications in the electronic structure of the Pt catalysts [13]. It has also been reported that graphene sheets strongly interact with Ru (0 0 0 1) surfaces by π–d hybridization. It is thus suggested in this study that Pt clusters of smaller size interact with graphene via the same type of π–d hybridization [14]. The difference between Pt/GNS and Pt/CB has been revealed by the extended X-ray absorption fine structure (EXAFS) measurements, which will be reported elsewhere. Further work is under way to clarify the mechanism of the CO tolerance for the Pt/GNS.

Acknowledgment

This work was supported by the New Energy and Industrial Technology Development Organization (NEDO), Japan.

References

[1] E.J. Yoo, J. Kim, E. Hosono, H.S. Zhou, T. Kudo, I. Honma, Nano Lett. 8 (2008) 2277–2282.
[2] S.M. Paek, E.J. Yoo, I. Honma, Nano Lett. 9 (2009) 72–75.
[3] Y. Gan, L. Sun, F. Banhart, Small 4 (2008) 587–591.

[4] R. Muszynski, B. Seger, P.V. Kamat, J. Phys. Chem. C 112 (2008) 5263–5266.
[5] C. Xu, X. Wang, J. Zhu, J. Phys. Chem. C 112 (2008) 19841–19845.
[6] Y. Si, E.T. Samulski, Chem. Mater. 20 (2008) 6792–6797.
[7] Y. Li, L. Tang, J. Li, Electrochem. Commun. 11 (2009) 846–849.
[8] E.J. Yoo, T. Okata, T. Akita, M. Kohyama, J. Nakamura, I. Honma, Nano Lett. 9 (2009) 2255–2259.
[9] W.S. Hummers, R.J. Offeman, J. Am. Chem. Soc. 80 (1958) 1339.
[10] H. Kita, H. Naohara, T. Nakato, S. Taguchi, A. Aramata, J. Electroanal. Chem. 386 (1995) 197–206.
[11] M. Sogaard, M. Odgaard, E.M. Skou, Solid State Ionics 145 (2001) 31–35.
[12] R. Kou, Y. Shao, D. Wang, M.H. Engelhard, J.H. Kwak, J. Wang, V.V. Viswanathan, C. Wang, Y. Lin, Y. Wang, I.A. Aksay, J. Liu, Electrochem. Commun. 11 (2009) 954–957.
[13] T. Kondo, K. Izumi, K. Watahiki, Y. Iwasaki, T. Suzuki, J. Nakamura, J. Phys. Chem. C 112 (2008) 15607–15610.
[14] S. Marchini, S. Gunther, J. Wintterlin, Phys. Rev. B 76 (2007), 075429-1-175429-.